Oblique, Stratified Winds about a Shelter Fence. Part I: Measurements

JOHN D. WILSON

Department of Earth and Atmospheric Sciences, University of Alberta, Edmonton, Alberta, Canada

(Manuscript received 23 September 2003, in final form 23 March 2004)

ABSTRACT

Wind statistics were measured using cup and sonic anemometers, placed upwind and downwind from a porous plastic windbreak fence (height $h = 1.25$ m, length $Y = 114$ m, resistance coefficient $k_{r0} = 2.4$, and porosity $p = 0.45$) standing on otherwise uniform land (short grass with roughness length $z_0 \sim 1.9$ cm). Intercomparison with collocated two-dimensional sonic anemometers suggested that, except in strongly stratified winds, cup anemometers (distance constant 1.5 m), subjected to a uniform overspeeding correction (here ~10%), provide a reasonably accurate transect of the mean wind across the disturbed flow region. The measurements, binned with respect to mean wind direction and stratification, establish that the resistance coefficient of a windbreak of this type implies the maximum (or ''potential'') mean wind reduction, a potential that is realized in neutral, perpendicular flow and for which a semiempirical formula is derived. Obliquity of the approaching wind *reduces* actual shelter effectiveness below the potential value, as was already known. However, a systematic influence of stratification could only be discriminated in winds that were not too far (say, within about $\pm 30°$) from perpendicular, under which conditions both stable and unstable stratification *reduced* shelter effectiveness. The ''quiet zone,'' in which velocity standard deviations (σ_u, σ_v) are reduced relative to the approach flow, was found to extend farther downwind for the normal velocity component (u) than for the parallel component (v).

1. Introduction

Like other disturbances of the atmospheric surface layer such as the step in surface roughness length or in surface energy fluxes, the well-defined shelter in the vicinity of a windbreak provides a useful criterion for wind models. Thirty years ago, when the capability to compute disturbances to the wind on the micrometeorological scale using the Reynolds-averaged Navier–Stokes (RANS) equations was quite new and optimism surrounded the introduction of second-order turbulence closures, Seginer (1975a,b) anticipated that his measurements of winds obliquely incident on a 50% porous windbreak fence ''may be used to check on calculational results of flow around windbreaks.'' Early computations for normally incident winds (Wilson 1985) were promising, and Wang and Takle's (1996) simulations of the impact of wind obliquity on the ''sheltered distance'' compared remarkably well with Seginer's observations. However Wilson and Yee (2003), testing RANS models against observations of wind about an array of barriers, found none of the common first- and second-order closures performed very credibly.

Taking a wider context, one might hypothesize from reading the literature that the surface-layer wind, however it may have been disturbed, is *obligingly* computable, because we frequently see reports of good agreement between measurements and wind models. The present shelter measurements, and the subsequent analysis and computations, aim to answer critically the following questions. May we say disturbed winds about a shelter fence are objectively computable, with today's RANS models? May we infer that a few dispersed point measurements of the mean wind and turbulence, acting as confirmation of a numerical simulation designed to extrapolate from those few measurements across the whole flow, provide sufficient detail to justify claiming that the flow disturbance is ''known,'' in the statistical sense? For if so we have at hand (in RANS models) a tool to ease the burden of measurements in wind-related studies, and, generalizing to other flow disturbances, a ''yes'' would suggest we can soon expect a generation of, for example, air-pollution models that take account of surface inhomogeneity in a more objective and credible way than at present.

This paper (Part I) describes new measurements of wind reduction when the winds, obliquely incident, encounter a long, straight porous fence. The observations go a little beyond those of Seginer in that they cover stable (as well as neutral and unstable) thermal stratification and in that the resistance coefficient of the fence (k_{r0}) is here known. Wilson (2004, hereinafter Part II) investigates whether the salient features of the observations are reflected in RANS wind models, using second-order closure.

Corresponding author address: John D. Wilson, Department of Earth and Atmospheric Sciences, 1-26 Earth Sciences Bldg., University of Alberta, Edmonton T6G 2E3 AB, Canada.
E-mail: jaydee.uu@ualberta.ca

Background on shelter flow

The effects of a long, straight, isolated, porous fence on a neutrally stratified and perpendicular wind will be familiar to many readers and may be quickly gleaned from articles by Raine and Stevenson (1977) and McNaughton (1988, 1989). In short, drag (i.e., momentum lost to the fence) results in a region of mean velocity reduction near ground and spanning roughly $-5 \leq x/h \leq 30$, while the deflection of a fraction of the approaching stream up and over the barrier results in a jet aloft, the enhanced shear between these regions resulting in strong shear production of turbulence. The resultant elevated mixing layer spurs reacceleration of the sluggish wake flow beneath and dictates that, except in its immediate lee, the windbreak results in *increased* turbulence. As for the ''quiet zone,'' that is, the ground-based, near-lee zone in which turbulence as well as mean wind is reduced, the agency for the reduced turbulence is the fluctuating drag on the fence, which extracts energy from the gusts and redeposits that energy into quickly damped, predominantly finescale eddies. These qualitative effects of the fence are implicit in the governing differential equations [see brief reviews by Wilson and Yee (2003) and by Wilson and Flesch (2003) for the computational perspective].

2. Details of the experiment and anemometers

The windbreak measurements were gathered during 22–30 May 2003, at the Ellerslie Research Station of the University of Alberta. A 45% porous, thin plastic windbreak fence (Tensar Corporation) of height $h = 1.25$ m and length $Y = 114$ m was erected in a large flat field of grass. It was held upright by posts spaced on irregular intervals of about 3–4 m, and, although (depending on the strength of the wind) the top of the fence bowed out of line between neighboring posts by as much as 10–15 cm, the rigidity of the plastic prevented fluttering. An image of the mesh (elliptical pores with semimajor and semiminor axis lengths of about 23 and 5 mm) is given in Part II.

A GPS unit was used to establish distant landmarks allowing one to align the fence north–south (y axis) and to orient the sensors determining wind direction. The mean wind direction corresponding to a wind from the west will be denoted in the usual compass convention as $\beta = 270°$, and for convenience β' will be denote the deviation of mean wind direction away from 270°.

The windbreak was of the same material as that used by Wilson (1997) in the same general configuration to study the windbreak pressure field, and by Argete and Wilson (1989), Zhuang and Wilson (1994), and Wilson and Flesch (2003) in other configurations. Its resistance coefficient, defined as $k_{r0} = \Delta P/(\rho U^2)$ [where ΔP is the pressure drop induced when the material blocks a uniform perpendicular stream with velocity U and density ρ (Laws and Livesey 1978)], had earlier been determined in the wind tunnel, where seven measurements covering $5.31 \leq U \leq 9.6$ m s^{-1} gave estimates in the range $2.36 \leq k_r \leq 2.41$. [Zhuang and Wilson wrongly cited the resistance coefficient of this, the Tensar plastic fence, as $k_{r0} = 1.66$, which on the contrary is the proper value of k_{r0} for the windbreak cloth used by McAneney and Judd (1987); both materials had been studied in the wind tunnel over the same few days.]

A 6-m mast placed 15 m (12h) west of the midline of the fence supported four cup anemometers (Climet, Inc., 011-4; distance constant 1.5 m; nominal starting speed 27 cm s^{-1}) paired with four two-dimensional (2D) sonic anemometers (Vaisala, Inc., WS425), at heights $z = 0.62$, 1.57, 3.07, and 5.02 m. The mast also supported a 3D sonic anemometer (Campbell Scientific, Inc., CSAT3) at $z = 2.00$ m, a wind vane at $z = 1.35$ m (the ''dead band'' of its rotary potentiometer being oriented so that the 360°/0° ambiguity corresponded to a north wind, that is, a wind parallel to the windbreak and thus of little interest), and two shielded and ventilated thermocouple pairs giving temperature differences between three levels $z = 0.34$, 1.31, and 4.25 m. Winds from the compass range covering from SSW through W to NNW approached the tower with a minimum uniform fetch of 400 m, so that the instruments on the tower determine the state of an undisturbed surface layer (Figs. 1, 2).

More cup and 2D sonic anemometers were arranged along a transect normal to the fence, that is, due E–W and defining the x axis. The intersection of this transect with the fence will be taken to define the coordinate origin $x = y = 0$. The transect lay 72 m (57.6h) south from the north end of the fence and thus 42 m (33.6h) north from the south end; the y coordinates of the north and south ends of the fence are $y/h = +57.6$ and -33.6, respectively. All instruments on the transect were placed at the same height $z = 0.62$ m as the lowest anemometer on the mast, that is, $z/h = 1/2$. Measurement locations along the transect are given in Table 1, and note that at several x/h sonic anemometers again were paired with cups. The rationale for placing *two* 2D sonic anemometers at $x/h = 15$ but widely separated on the y axis was that significant difference between wind statistics from these two spots would indicate inhomogeneity on the y axis, that is, would signal end effects. This capability is useful because in this work the observations are interpreted under an a priori assumption of homogeneity on the y axis. For mean wind directions as far as $\beta' = 60°$ from normal, no sign of inhomogeneity was seen by the paired 2D sonic anemometers at $x/h = 15$ (of course at larger x/h, end effects must come into play). A second 3D sonic anemometer was also operated in the lee, at $x/h = 2$ or 10, $z/h = 1$, and $y/h = 10$.

Data acquisition was handled by three Campbell Scientific (CSI) dataloggers, whose clocks were synchronized to better than 1 s: a CR7, counting pulses from the cup anemometers (one per revolution, 1-min totals averaged over 15 min) and logging the analog signals

FIG. 1. Windbreak experiment at Ellerslie, AB, Canada. A view to the west, showing the uniform upwind fetch for the shelter measurements and paired cup and 2D sonic anemometers on the mast.

from the thermocouples and the wind vane at intervals $\Delta t = 1$ s; a CR23X running the eight 2D sonic anemometers with sampling interval $\Delta t = 8$ s (an appendix discusses the implications of this slow sampling rate on velocity statistics derived from the 2D sonic anemometers); and a CR10X running the 3D sonic anemometers ($\Delta t = 0.1$ s). These signals were recorded semicontinuously over 22–30 May, and a total of almost three hundred 15-min records having a mean wind direction within $\pm 60°$ from due west ($210° \leq \beta \leq 330°$) permitted a detailed examination of the winds about the fence, as a function of orientation of the mean wind and in relation to stratification. At the end of the measurement interval the grass was 15–20 cm tall, not having greatly changed over the preceding 9 days. No time trend was seen in the surface roughness length, and an estimate $z_0 = 1.9$ cm (standard error 0.07 cm) was deduced by best-fitting Monin–Obukhov (MO) profiles, as an average over 60 periods having mean speed from the 2D sonic anemometer at $z = 0.62$ m above 1.5 m s^{-1}, friction velocity from the upwind 3D sonic anemometer above 0.2 m s^{-1}, magnitude of the Obukhov length L from the 3D sonic anemometer exceeding 50 m, and mean wind direction $225° \leq \beta \leq 315°$.

a. Comparative performance of anemometers in undisturbed wind

Repeated individual wind-tunnel calibrations of the Climet cups, over several years, have determined that their steady-state response is universal ($s = 0.025C + 0.25$, where s is the 1-min mean speed and C is the number of rotations) in a wind above 1 m s^{-1}, provided the bearings are in good order (they are exceptionally durable and can easily be checked because the cup assembly is removable) and that the cup assembly is in prime condition. Calibration of the 2D sonic anemometers was provisionally assumed to be unnecessary because they had been delivered only weeks before the experiment.

To compare the upwind cup and sonic anemometers, the observations were filtered (to avoid periods of cup stalling, etc.) according to the requirements that mean speed from the 2D sonic at $z = 0.62$ m must exceed 1 m s^{-1}, that the friction velocity from the upwind 3D sonic must exceed 0.1 m s^{-1}, that the magnitude of the Obukhov length from the 3D sonic should exceed 1 m, and that the mean wind direction $225° \leq \beta \leq 315°$ (to avoid any risk of flow off the fence). Figure 3 gives the

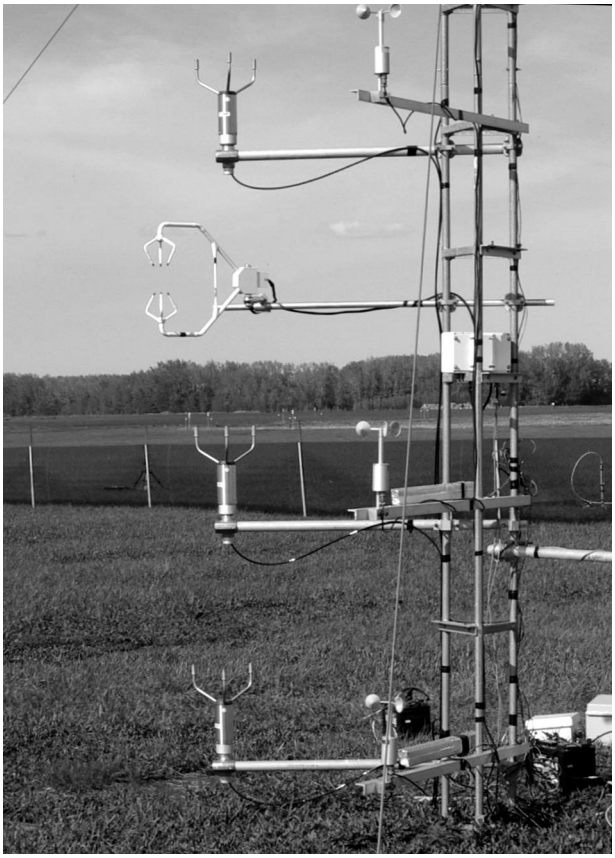

FIG. 2. Windbreak experiment at Ellerslie. A view to the northeast, showing the plastic fence (height $h = 1.25$ m and porosity $p = 0.45$), the CSI 3D sonic anemometer (centered at $z = 2$ m), and thermometer intake shields. Periods with winds approaching the tower from this direction were discarded.

resulting ensemble of 15-min mean overspeed ratios S_{cup}/S_{son} on the upwind tower as a function of local z/L. What is evident is that these selective data do not indicate a strong correlation of S_{cup}/S_{son} against z/L at any level, that overspeed ratios are more scattered below than above 2 m, and that S_{cup}/S_{son} is in general distinctly larger, at the lowest level. The extreme outlier in Fig. 3, an overspeeding factor of 1.30 from the reference cup anemometer (which registered 1.67 m s^{-1} as opposed to the 1.28 m s^{-1} from the paired sonic anemometer),

TABLE 1. Locations of anemometers on transect at $z/h = 1/2$ across the windbreak.

x/h	y/h	Type
−12	0	Cup and 2D
−2 or −1	0	Cup
2	0	Cup
4	0	Cup and 2D
6	0	Cup
10	0	Cup and 2D
15	0	Cup and 2D
15	+11	2D
20	0	Cup

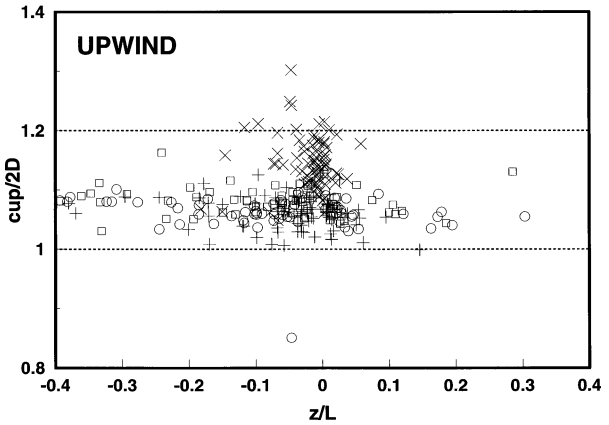

FIG. 3. Ratio of wind speed measured by cup anemometer to wind speed measured by 2D sonic anemometer, at four levels in the upwind (equilibrium) surface layer (×, +, □, ○ in ascending order on the mast, $z = 0.62$, 1.57, 3.07, 5.02 m). Selection criteria are given in text.

occurred during 0745–0800 mountain daylight time (MDT), with $u_* = 0.17$ m s^{-1}, $L = -13$ m, and all six wind directions on the mast in the range 286°–290°. Possibly this (excessive) overspeeding factor is due to a sampling fluctuation in the mean wind speed as determined by the 2D sonic anemometer, because (as explained in the appendix) wind statistics from the 2D sonic anemometers were subject to significant sampling error because of the low sampling rate.

Figure 4a is a statistical comparison of the shapes of

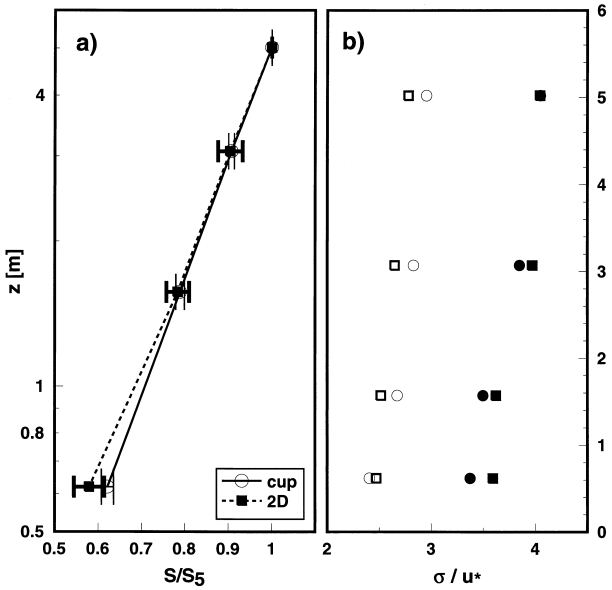

FIG. 4. Upwind profiles of normalized velocity statistics: (a) mean wind speed according to the cup and 2D sonic anemometers [avg and std dev of 29 cases ($|L| \geq 100$ m; $S_{0.2D} \geq 1$ m s^{-1})]; (b) ensemble mean profiles, under neutral ($|L| > 180$ m) and under unstable ($-11 \leq L \leq 8$ m) stratification, of the std devs σ_u (circles) and σ_v (squares) from the 2D sonic anemometers normalized (prior to ensemble averaging) on the friction velocity from the 3D sonic anemometer.

TABLE 2. Fifteen-minute mean wind speeds (m s^{-1}) from the cup anemometers (uncorrected) and 2D sonic anemometers, exposed along a transect at the specified distances *east* of the windbreak, for periods of due *east* wind (L and u_* cannot be cited, because mast lay downwind of fence). Variability of the computed overspeeding factors in this uniform flow likely stems from individual biases of the 2D sonic anemometers.

							Sonics			
Day	t_{end}	4 h	6 h	10 h	15 h	20 h	4 h	10 h	15 h	15 h
145	1815	1.73	1.75	1.72	1.80	1.84	1.50	1.49	1.51	1.57
145	2045	2.35	2.28	2.31	2.34	2.31	2.08	2.06	2.15	2.26
149	2100	2.37	2.41	2.31	2.28	2.27	2.31	2.36	2.45	2.52
Avg		2.15	2.15	2.11	2.14	2.14	1.96	1.97	2.04	2.12
Overspeed		10%		7%	1%–5%					

the mean wind profile, according to the cup and 2D sonic anemometers, in near-neutral stratification. Selected individual profiles were normalized by wind speed (cup or sonic anemometer as appropriate) at the highest level (S_5), and the normalized profiles were averaged. The first point to be made is the unimpeachable quality of the cup profiles—virtually a perfect straight-line relationship of S/S_5 versus ln(z), with very small standard deviation (the standard deviation need not vanish, for the 29 cases selected cover the stability range $|L| = 100$ m $\rightarrow \infty$). Second, we note that the standard deviations for the 2D sonic anemometers are 3–4 times those for the cup anemometers (a likely reason for this result is discussed in the appendix). Last, having seen from Fig. 3 that the 2D sonic anemometer at the lowest level reads *especially* much lower than its companion cup anemometer, we can now conclude that it (the 2D sonic anemometer) is out of calibration because Fig. 4 establishes that the 2D sonic anemometer's reported wind speed at this lowest point on the mean wind speed profiles does not fall on the expected straight line of S/S_5 versus ln(z). Hence velocity statistics from the ''reference'' 2D sonic anemometer (the lowest on the mast, at $z = 0.62$ m) have been multiplied by the factor $r = 1.07$, which brings the mean normalized wind speed at that level onto the expected straight line. Upon accepting that correction, we may conclude that an overspeeding factor of 8% is about right for the cup anemometers in undisturbed flow, irrespective of height and stability. This is the correction previously employed by Wilson and Flesch (2003), here arrived at by an alternative and more convincing means; cup data shown here (and in part II) have been corrected by 10%.

It is desirable also to develop some confidence in the other anemometers arrayed about the wind break ($z = 0.62$ m, $z/h = 0.5$). Several 15-min periods with winds from due east allowed a check of their uniformity of response in an undisturbed wind (the surface to the east of the fence matched that upwind out to about 200 m, beyond which the field, still flat, was in low stubble). Table 2, a selection of three 15-min intervals during which the mean wind lay within 3° of due east, provides convincing evidence of the uniform response of the cup anemometers but suggests individual biases in the 2D sonic anemometers (note: no bias corrections have been applied to these leeward sonic anemometers).

Still on the matter of anemometer performance, and because in a following section (3g) the level of turbulence in the lee of the windbreak will be examined on the basis of the 2D sonic anemometers, it is necessary to establish the plausibility of turbulence statistics from the latter, in the upwind (undisturbed) flow. Figure 4b shows ensemble-averaged upwind profiles of normalized velocity standard deviations σ_u/u_* and σ_v/u_*, derived from the 2D sonic anemometers (u_* from the 3D sonic anemometer) over 12 near-neutral periods ($|L| >$ 180 m) and over 8 unstable periods ($-11 \leq L \leq -8$ m); here, as everywhere in this paper, u and v are the velocity components respectively perpendicular and parallel to the fence, and thus, one's accustomed expectations as to the relative magnitudes of σ_u and σ_v, with u oriented along the mean wind, do not apply. Selection criteria for these data were $S_0 \geq 1$ m s^{-1}, $u_* \geq 0.1$ m s^{-1}, and $225° \leq \beta \leq 315°$.

The weak height gradient under neutral stratification may be surprising, given that Monin–Obukhov similarity theory (MOST) posits that σ_u and σ_v do not vary with height (i.e., $z/L \rightarrow 0$ in neutral stratification). However, MOST specifically applies to the layer $z_0 \ll z \ll \delta$ (where δ is depth of the boundary layer), that is, is not expected to be valid close to ground. Much of the familiar data on profiles of σ_u and σ_v stems from much taller towers than the present one, and so these height gradients in Fig. 4b may reflect the necessary dependence on z/z_0 for small z. It is significant to note that even with the averaging together of individual runs to create an ensemble average over 2 h, the normalized profiles remain a little ragged. However, magnitudes $\sigma_u/u_* \approx \sigma_v/u_* \approx 3$ and ≈ 4 are plausible for (respectively) the neutral and the moderately unstable surface layer. A comparison (not shown) of upwind standard deviations σ_u and σ_v reported by the 2D sonic anemometers (at $z = 1.57$ = and 3.07 m) against those from the 3D sonic anemometer (at $z = 2$ m) evidenced no overall bias (values from the two 2D sensors were linearly interpolated to the height of the 3D sensor). Individual random differences, however, were sizeable: fractional differences $\delta_u = |\sigma_u^{2D} - \sigma_u^{3D}|/\sigma_u^{3D}$ (and similar for δ_v)

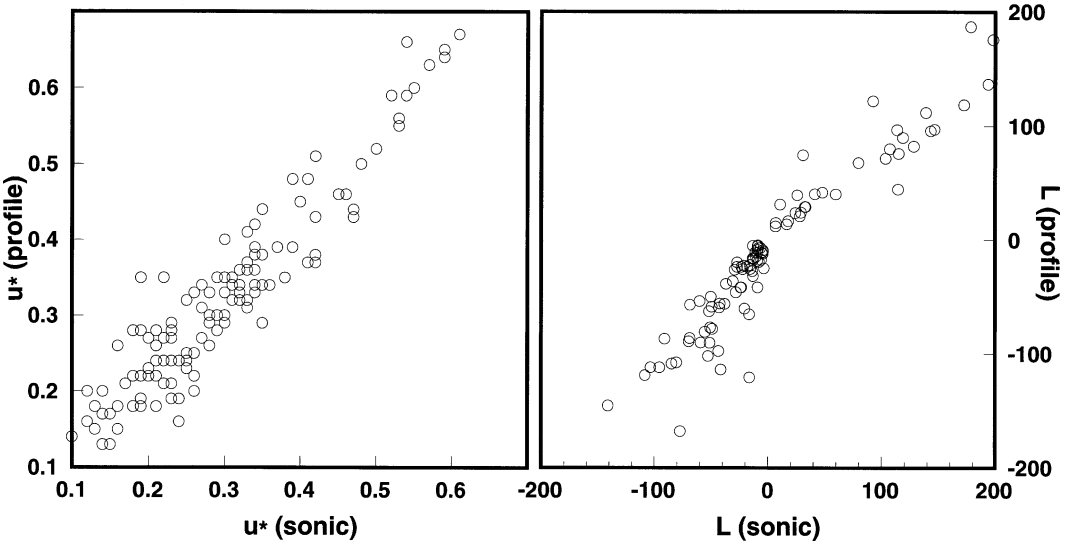

FIG. 5. Comparison of MOST scales as deduced from profiles and as directly measured by the 3D sonic anemometer (data-selection filter given in text; scale for L renders invisible all $|L| > 200$ m). Best-fit slope for u_* is 1.001; best-fit slope for L is 0.95 (L–L data pairs containing either $|L| > 200$ m rejected for the regression).

were computed for 67 cases ($S_0 \geq 1$ m s^{-1}, $u_* \geq 0.1$ m s^{-1}, $|L| \geq 2$ m, and $|\beta'| \leq 45°$), and for both components the standard deviation of those fractional differences was about 0.1.

b. Wind direction signals

Up to 11 wind direction signals were available, 6 of them pertaining to the upwind flow: wind direction was available from the four 2D sonic anemometers on the mast, from the 3D sonic anemometer at $z = 2.00$ m, and from a wind vane at $z = 1.35$ m. This wealth of information proved to be interesting and useful: for the majority of 15-min periods, the six upwind mean wind directions were consistent, to within $\pm 10°$ or better, yet there were some intervals during which unaccountable differences between them were seen. These differences may have been intervals during which large swings in wind direction transiently rendered the nominally ''upwind'' region instead *downwind* of the fence. To avoid being confused by such effects, data were rejected from the analysis unless $|\beta_v - \beta_{3D}| < 10°$, where β_v is the mean wind direction from the vane and $\beta_{3D} = \text{atan}(\overline{v}/\overline{u})$ is the direction of the mean wind according to the upwind 3D sonic-anemometer.

c. Governing scales for the upwind surface layer

A correlation plot (not shown) of the measured temperature differences on the upwind mast ($\overline{\Delta T}$) against the temperature scale $T_*(=-\overline{w'T'}/u_*)$ provided by the 3D sonic anemometer correctly trended through the origin, confirming the absence of electronic voltage offsets. Radiation errors in the $\overline{\Delta T}$ ought to have been small, because of the provision of a polyvinyl chloride (PVC) shield wrapped in reflective tape and because of strong ventilation ($\sim$4 m s^{-1}). Thus, best-fit MOST profiles were conformed to the profiles of wind speed and temperature (cups and thermocouples), following the same scheme as Argete and Wilson (1989), and using the MO functions (ϕ_m and ϕ_h for wind and temperature) recommended by Dyer and Bradley (1982). Figure 5 indicates that, for periods with $u_* \geq 0.1$ m s^{-1}, $L \geq 1$ m, and $225° \leq \beta \leq 315°$, the profile-derived friction velocity and Obukhov length were in reasonably good agreement with corresponding values measured directly by the 3D sonic anemometer–thermometer. Sonic friction velocity was computed as $u_* = (\overline{u'w'}^2 + \overline{v'w'}^2)^{1/4}$, and sonic temperature was used to compute the vertical heat flux (mean vertical velocity from the 3D sonic anemometer was always small, and although a coordinate rotation $\overline{w} \rightarrow 0$ was nevertheless performed, it had practically no effect). A linear regression gave a perfect slope (1.001) for the relationship between profile and sonic friction velocities, but the scatter about the 1:1 line and the fact that the average ratio $u_*^{\text{tow}}/u_*^{\text{son}} = 1.10$ (standard deviation 0.018) raise the question (not pursued here) as to which would be the better estimate of u_* with which to scale observed velocity statistics.

What Fig. 5 does not convey is that sonic-derived and profile-derived surface-layer parameters may greatly differ during periods of very light winds (generally associated with extreme stratification). A bulk Richardson number was computed for each run from the upwind tower observations, namely,

$$\text{Ri}_b = \frac{g}{T_0}\frac{\Delta\overline{T}\Delta z}{(S_5)^2}, \tag{1}$$

where $\Delta\overline{T} = \overline{T}(4.25) - \overline{T}(0.34)$, $\Delta z = (4.25 - 0.34)$

m, and S_5 is the (overspeeding corrected) cup wind speed at $z = 5.02$ m. During conditions of extreme stratification, Ri_b proved to be a more reliable diagnostic (and basis for classification) than stability parameters (T_*, L) derived from the 3D sonic anemometer.

3. Analysis of the measured shelter

In order that any given 15-min record be accepted for the wind speed transects to follow, overspeeding-corrected cup wind speed (S_0) at the lowest level on the tower ($z = h/2 = 0.62$ m) was required to exceed 1 m s^{-1} and friction velocity from the 3D sonic anemometer was required to exceed 0.1 m s^{-1} [the latter criterion bears on the stability classification of, but not directly on the accuracy of, the cup wind speed transects $S(x)/S_0$]. The mean wind direction (β_v) from the vane was required to be within $\pm 10°$ of the desired angle of obliquity relative to the normal to the windbreak (0°, 30°, or 60°), and the vane and the 3D sonic anemometer [$\beta_{3D} = \mathrm{atan}(\overline{v}/\overline{u})$] were required to give orientations that were consistent to within $\pm 10°$ (usually they were within 5°). Furthermore, in defining the relative cup wind speeds, the reading from any downwind cup reporting a mean speed of less than 1 m s^{-1} was ignored, to avoid being confounded by intervals of cup stalling. Cited values of u_*, and L are those indicated by the 3D sonic anemometer.

For the following discussion it will be convenient (and may lend clarity) to introduce a symbol Δ_S for the fractional reduction in mean wind speed, which is a function of location and of the orientation and stratification of the incident mean flow

$$\Delta_S(x, z; \beta', L) \equiv \frac{S_0(z) - S(x, z)}{S_0(z)}. \tag{2}$$

Where there is no danger of confusion, Δ_S will be used interchangeably with $\Delta S/S_0$; the argument z may sometimes be dropped on the approximation that $\Delta S/S_0$ is (roughly) height independent for $z/h \lesssim 1/2$ in the near lee (Heisler and Dewalle 1988). By definition, $\Delta_S(\check{x}; \beta', L)$ will be the *amplitude* (or ''depth'') of the curve $S(x)/S_0$ of relative mean wind speed (at $z/h = 1/2$), with $\check{x}$ being the location at which minimum wind speed occurs.

a. Wind speed transects for perpendicular incidence

The case of a neutrally stratified surface-layer wind at perpendicular incidence to a straight fence is the simplest real case of windbreak flow, amply explored experimentally (e.g., Seginer 1975b; Bradley and Mulhearn 1983; Wilson 1987, 1997) and, according to previous reports, very well simulated by numerical models, irrespective of the sophistication of their closure. The early simulations by Wilson (1985), which were in very good accord with the Bradley–Mulhearn observations,[1] established that fractional wind reduction is not very sensitive to the parameter h/z_0 and yielded a formula (Wilson et al. 1990) for the amplitude of the relative wind curve in neutral and perpendicular flow,

$$\Delta_S(\check{x}; 0, \infty) = \frac{k_{r0}}{(1 + 2k_{r0})^{0.8}}. \tag{3}$$

For the plastic windbreak of the current study, $k_{r0} = 2.4$, and Eq. (3) implies that (in neutral and perpendicular winds) one may expect the trough in the relative wind curve to base out at $(S/S_0)^{\min} = 1 - \Delta_S(\check{x}; 0, \infty) = 0.41$; that is, mean wind speed reduced to only 41% of the value in the open.

Figure 6 gives the relative wind transects S/S_0 of the experiment, for nearly perpendicular incidence ($260° \leq \beta \leq 280°$). The single period of perpendicular and ''neutral'' winds ($u_* = 0.22$ m s^{-1}, $L = -137$ m, and $\beta_v = 278°$) occurred only 2 h after the commencement of data collection (1800–1815 MDT 22 May) during the evening transition, for over the previous and subsequent 15-min intervals, respectively, $L = -77$, and $+31$ m. Given that the wind was strong and perpendicular (directions of the mean wind upwind and downwind, according to the 3D sonic anemometers, were $\beta_{3D} = 273°$ and 277°, respectively; leeward 2D sonic anemometers were not yet in operation, but those on the tower reported $\beta = 276°$, 276°, 279°, and 277°), it seems unwarranted to reject the wind reduction data from this run on the sole basis of nonstationarity of the heat flux [notwithstanding the warning issued by Bradley and Mulhearn (1983)]. The single period of stable stratification, for which $\beta = 287°$, was immediately subsequent to the neutral run; it has been admitted by relaxing the criterion for normality.[2] The most unstable run, for which according to the 3D sonic anemometer, $u_* = 0.097$ m s^{-1}, and $L = -0.7$ m, has been permitted its slight transgression of the criterion $u_* \geq 0.1$ m s^{-1} owing to its adequate

[1] Turbulence closures and the numerical method were standard; all physical parameters (h, z_0, and k_r) were fixed and known, a priori. Only in regard to numerical parameters, such as domain size and resolution, was there flexibility. However, in Part II it is shown that these first simulations were subject to a more substantial discretization error than originally appreciated.

[2] Figure 12 shows that sensitivity of mean wind reduction to the obliquity of the approach flow is weakest for nearly perpendicular winds, but nevertheless there is some danger of confounding the influences of obliquity and stability in accepting this run. Anticipating later results, according to Eq. (8) at 17° obliquity (i.e., with $\beta = 287°$) the fractional wind reduction (at $x/h = 4$) will be 96% of the value $\Delta_S(\check{x}; 0, \infty) = 0.57$ observed in neutral and perpendicular flow, namely $\Delta_S = \Delta S/S_0) = 0.55$; however, the observed fractional reduction ($\Delta S/S_0 = 0.48$) due to the combined effects of obliquity and stability is only 84% of that observed in neutral, perpendicular flow. On this evidence one may postulate that the effect of stable stratification on fractional wind reduction has the same sign as the effect of obliquity, that is, results in less effective shelter. The same suggestion is reached by using Seginer's (1975b) empirical formula for the obliquity effect on a (similar) fence in neutral flow, to extract the influence of obliquity from this run ($\beta' = 17°$, $L = 31$ m).

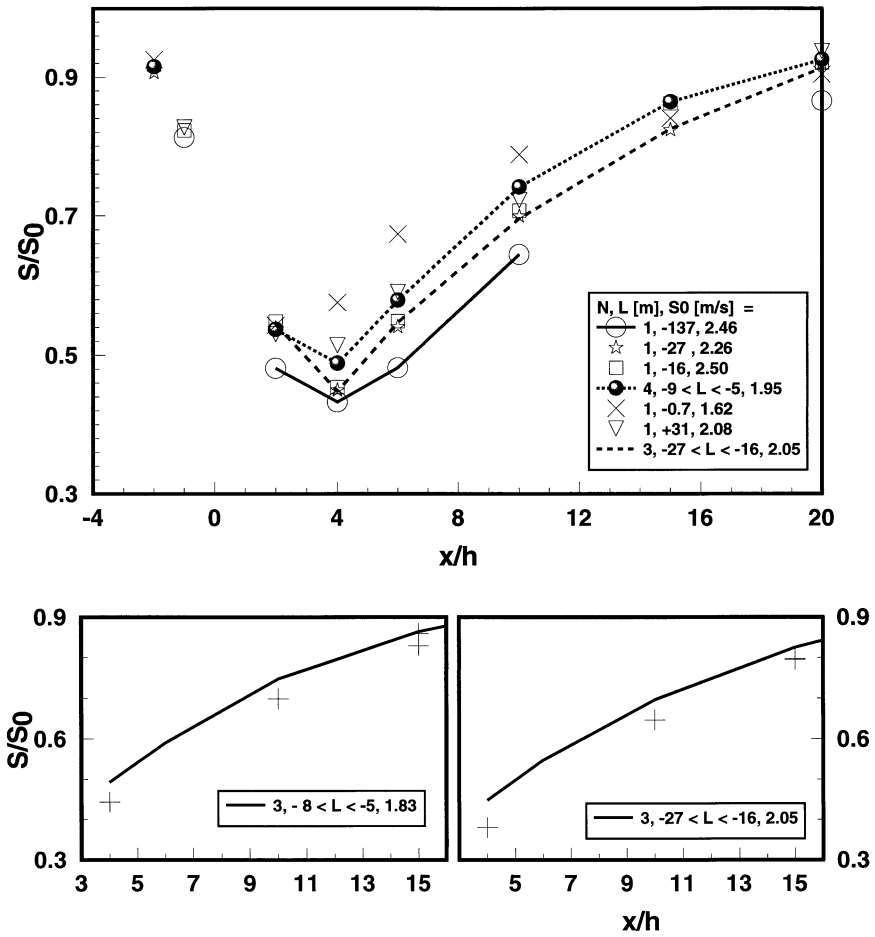

FIG. 6. Transects of relative wind speed S/S_0 at $z/h = 1/2$, for nearly perpendicular mean winds ($\beta = 270° \pm 10°$). (top) Transects from the cup anemometers alone; (bottom) selected cup transects (lines) compared with simultaneous transects from the 2D sonic anemometers. Legend (here and elsewhere) gives the number of 15-min intervals averaged together, the range in L covered, and the mean cup reference wind speed (S_0; corrected cup wind speed at $z = 0.62$ m $= h/2$ on the upwind mast) over the interval. Among all runs included (individually or in ensemble), the lowest reference wind speed was $S_0 = 1.53$ m s^{-1}. Directional selectivity was relaxed to admit the single run under stable stratification, for which $\beta = 287°$.

''windiness'' as judged by mean cup speeds; however, one ought to consider its classification with regard to u_* and L as qualitative (only), and (in view of the small u_*) perhaps cup stalling could have occurred even though mean cup speed $S_0 \geq 1$ m s^{-1}.

For the neutral condition, the minimum relative windspeed is $(S/S_0)^{\min} \approx 0.43$, that is, $\Delta_S(\check{x}; 0, \infty) \approx 0.57$. Thus Eq. (3) nicely diagnoses the depth of the trough in the relative wind curve, given the measured value of k_{r0}, as has been noted in other cases. Looking at this the other way around, if we take the measured $(S/S_0)^{\min} \approx 0.43$ and compute from it an effective resistance coefficient with Eq. (3), we obtain $k_{r0}^{\text{eff}} \approx 2.2$, which is close to the true value (as determined in the wind tunnel).

In regard to the impact of stratification, according to Fig. 6 the influence of instability is to lessen systematically the effectiveness of the windbreak in that higher relative wind speeds are seen in the entire leeward region than in the reference (neutral) case; in extreme instability, the location of lowest observed wind speed ($\check{x}/h$) moves closer to the fence. These effects were expected, on the basis of the earlier findings of Seginer (1975a), and so the sole surprise in Fig. 6 is the impact of *stable* stratification, which apparently also *lessens* shelter effectiveness.

The lower part of Fig. 6 compares transects from the cup and the 2D sonic anemometers (no comparison for the neutral case is made, because the leeward 2D sonic anemometers were not yet in operation). Recalling that a uniform 10% overspeeding correction will vanish in ratios S/S_0, Fig. 6 suggests that the leeward cups overspeed by *more* than 10% (''excess overspeeding'') in moderately and very unstable stratification. Although

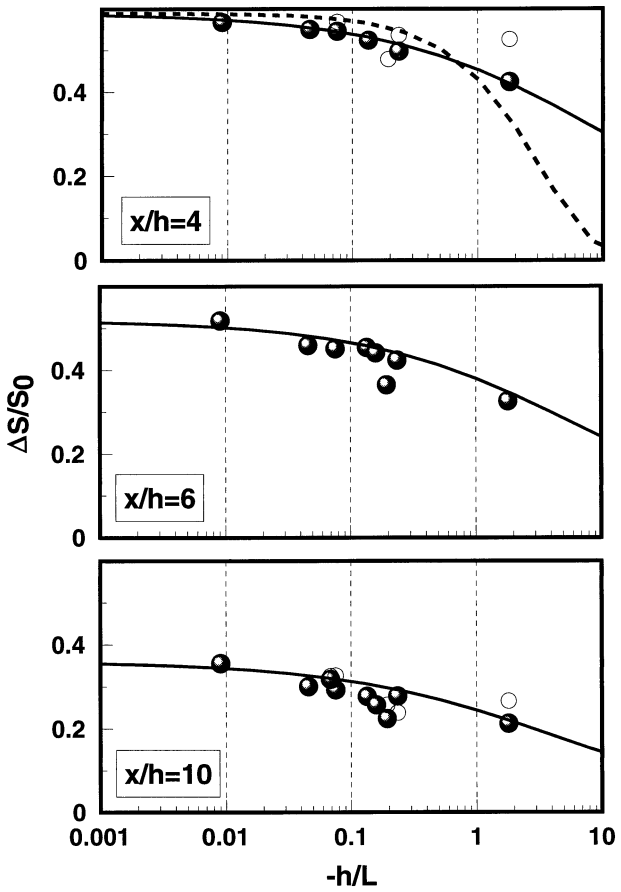

FIG. 7. Stability sensitivity of the fractional wind speed reduction $\Delta S/S_0$ at $x/h = (4, 6, 10)$ for winds at perpendicular incidence (15-min means, and from unstable side only; organization against Ri_b and against h/L about equally effective); solid symbols for cup anemometers, and open symbols for 2D sonic anemometers. The solid line is Eq. (4), and the dashed line is Eq. (5), the formulation of Seginer (1975a).

this is plausible, the cup wind speed transects shown throughout the paper have *not* been adjusted to attempt a compensation for possible *excess* overspeeding in the lee.

Figure 7 replots the observed fractional wind reduction at $x/h = (4, 6, 10)$ as a function of instability. The fitted curve is

$$\Delta_S(x;\, 0,\, L) = \frac{\Delta_S(x;\, 0,\, \infty)}{1 + a(x/h)^n(h/|L|)^n}, \qquad (4)$$

with $a = 0.15$ and $n = 1/2$. Recall that $\Delta_S(x;\, 0,\, \infty)$ is the maximum value of the fractional reduction for the given position x, that is, that observed in neutral stratification and perpendicular winds; also recall that for $x = \check{x}$ (i.e., $x/h \sim 4$) this is given by Eq. (3) as $\Delta_S(\check{x};\, 0,\, \infty) = (\Delta S/S_0)^{\max} = 0.59$. In selecting this formula it was desirable that the effect of shelter should vanish entirely as $|L| \to 0$, however there is otherwise no theoretical basis behind this particular fit. Also plotted for comparison in Fig. 7 is a stability correction suggested by Seginer (1975a) on the basis of a fit to his own similar shelter observations, namely,

$$\Delta_S(x;\, 0,\, L) = \Delta_S(x;\, 0,\, \infty)\, \exp\left(\alpha \frac{\phi_h}{\phi_m^2}\frac{h}{L}\right). \qquad (5)$$

In Eq. (5) the factor $\phi_h\phi_m^{-2}h/L$ has been substituted for Seginer's gradient Richardson number Ri_h, where ϕ_m and ϕ_h are the universal MO functions for the profiles of velocity and temperature. The dashed line in Fig. 7 was obtained by setting $\phi_h = \phi_m^2$ in Eq. (5) and specifying $\alpha = 0.31$, a value taken off Seginer's Fig. 9b for "anemometer 5" [which lay at $x/h = 5$, the location of minimum (observed) wind speed for his experiment]. It is evident that Seginer's formula for the influence of unstable stratification does not describe the current observations very well (though this suggestion hinges largely on one's acceptance of the cup anemometers' S/S_0 at $h/L = -2$). Using the Dyer and Bradley (1982) ϕ_h and ϕ_m in Eq. (5), that is, the ϕ_h and ϕ_m that have been used in the analysis of the Ellerslie experimental data and that do not have the convenient property that $\phi_h/\phi_m^2 = 1$, does not improve the fit. Note that Seginer found α (his stability sensitivity) to be minimal in the immediate lee ($x/h \sim 2$), still small at $x/h \approx 4$–5, and much larger in the farther lee. The current observations from near-normally incident flow do not show that trend.

If the influence of atmospheric stability on shelter flow was principally through the form of the approach profile, as it affects the mass flux of air impeded by the barrier, it would be implicit in the standard MO diabatic correction of the equilibrium wind profile, and thus one might posit that Eq. (3) for the fractional wind reduction ought to apply irrespective of stratification. The fact that it manifestly does not is presumably sign of a direct influence of stratification on the flow disturbance by the barrier.

b. Winds at 30° obliquity

Figure 8 gives transects of relative wind speed for periods during which the mean wind direction was oriented 30° ± 10° away from the normal to the fence. In weakly stratified winds, the cup and 2D sonic anemometer transects of S/S_0 are very consistent, but, in strongly stable stratification, cup overspeeding in the near lee apparently exceeded the corresponding figure (~10%) for equilibrium flow. In the neutral limit, relative wind speed at the most protected point in the near lee ($S/S_0 \approx 0.50$) is not diminished as strongly as is the case in perpendicular winds, as was evident from Seginer's and others' measurements. The influence of stratification at this angle of obliquity is less marked than in the case of perpendicular winds; that is, moderate stratification only slightly alters the relative wind curve. Of interest, however, and as in the case of perpendicular flow, both stable and unstable stratification are associated with *higher* wind speeds in the lee (less protection). A possible explanation is that, for oblique winds, a *directional*

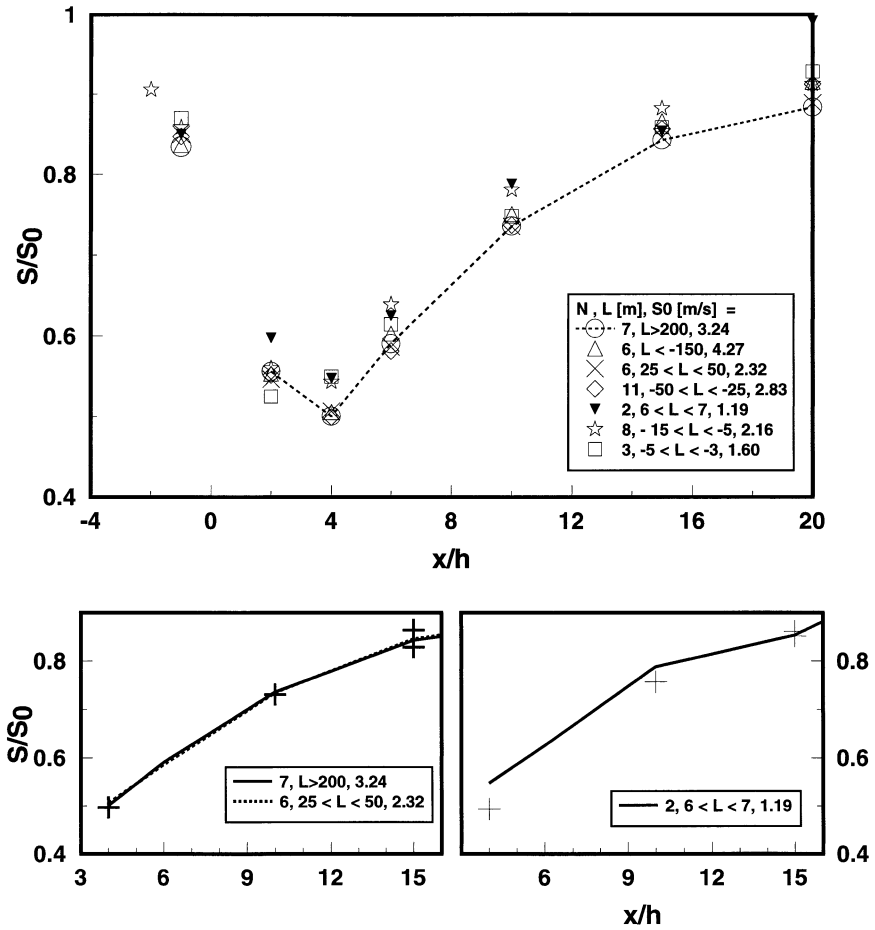

FIG. 8. Transects of relative wind speed S/S_0 at $z/h = 1/2$, for an approach wind direction 30° ± 10° away from the normal to the fence ($290° \leq \beta \leq 310°$ or $230° \leq \beta \leq 250°$). (top) Transects from the cup anemometers alone; (bottom) selected cup transects (lines) compared with simultaneous transects from the 2D sonic anemometers. Sonic data for the six periods with $25 \leq L \leq 50$ m are unavailable.

shear, that is, change in mean wind direction with height and with downwind distance, is necessarily created—in addition to the speed shear ($\partial S/\partial z$, $\partial S/\partial x$) that results from the resistance of the barrier. This effect should augment the rate of shear production of turbulent kinetic energy and therefore lessen the sensitivity of the mean flow pattern to upwind stratification.

In view of the fact that as a wind of given speed is deviated to strike a windbreak obliquely the resistance-generating normal component decreases, the wind reduction in slightly oblique flow might be expected to vary with cos β'; that is,

$$\Delta_S(x;\ \beta',\ L) = \Delta_S(x;\ 0,\ L)\ \cos\beta'. \qquad (6)$$

For the current fence ($k_{r0} = 2.4$), Eq. (3) implies that $\Delta_S(\check{x};\ 0,\ \infty) = 0.59$, and at 30° obliquity Eq. (6) accordingly specifies the best fractional reduction as $\Delta S/S_0 = 0.51$, so that at the trough of the relative wind curve $S/S_0 = 0.49$: this is very close to the mean wind reduction actually indicated by Fig. 8 in the neutral limit. An alternative (but, for small obliquity angles, *equivalent*) way to look at this [see also Richards et al. (1984)] is to note that for a sheet of material mounted such that its normal makes an inclination β' relative to the stream, the resistance coefficient is (Laws and Livesey 1978)

$$k_r(\beta') = k_{r0}\ \cos^2\beta', \qquad (7)$$

so that when the wind strikes the current fence (resistance coefficient $k_{r0} = 2.4$) at a 30° angle of obliquity, the *effective* resistance coefficient is $k_r(30°) = k_{r0}\ \cos^2(30) = 1.8$. Substituting this value into Eq. (3), one obtains an expected fractional reduction $\Delta S/S_0 = 0.53$, and the corresponding relative wind speed, at the point of best shelter, is $(S/S_0)^{\min} = 0.47$—again, in good agreement with the observations.

c. Winds at 60° obliquity

When the wind strikes the fence from a still more oblique angle of 60° ± 10° away from the normal to

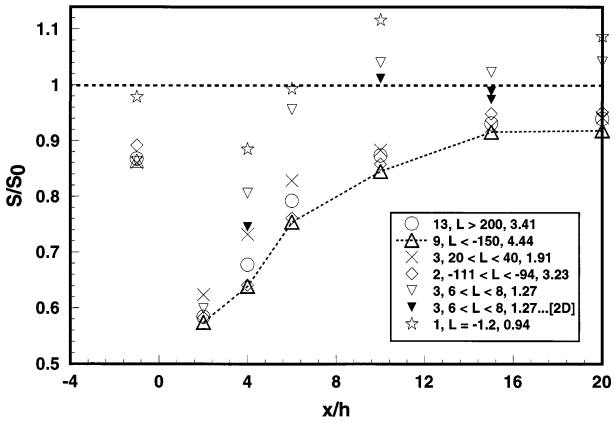

FIG. 9. Transects of relative wind speed S/S_0 at $z/h = 1/2$ from the cup anemometers (and in one case, also from the 2D sonic anemometers) for an approach wind direction $60° \pm 10°$ away from the normal to the fence ($320° \leq \beta \leq 340°$ or $200° \leq \beta \leq 220°$). The case $L = -1.2$ m does not satisfy the selection criterion on u_* and, as explained in the text, must be discounted. Note that the cup and sonic anemometer transects (compared for the ensemble of three cases $6 < L < 8$ m) differ in that the sonic anemometers do not indicate a convincing overshoot in the leeward wind speed.

the fence, shelter in the lee, as indicated (Fig. 9) by a trough in the relative cup anemometer wind speed, is still further compromised. In the neutral limit, $(S/S_0)^{\min} \approx 0.57$–$0.59$; that is, $\Delta S/S_0 \approx 0.41$–$0.43$. This is markedly better than the fractional wind reduction ($\Delta S/S_0 = 0.32$) suggested by either of the heuristic paths of the previous section, that is, by Eqs. (3) and (7) or Eq. (6). Strongly stable thermal stratification enhanced the leeward wind speed (reduced wind protection $\Delta S/S_0$), but no observations were obtained under unstable stratification, with $|\beta'| \sim 60°$.

In two of the cases shown, cup anemometer wind speeds exceeded the approach (reference) value in the middle and far lee. An (apparent) speedup (in the supposedly ''protected'' region at $z/h < 1$) has been termed ''overshoot'' by Jacobs and Wartena (1987) and was also reported by Nord (1991) in the case of a multiple-row tree windbreak (in which case it occurred even in near-neutral stratification). However, for the ensemble of runs with $6 \leq L \leq 8$ m (for each of which u_* is less than 0.12 m s^{-1}) the transect from the 2D sonic anemometers does not show the definite overshoot apparent in the corresponding cup anemometer transect, raising the possibility that the overshoot is spurious, a fiction of the (incorrect) response of the cup anemometers. The run identified as $L = -1.2$ m, which shows a very marked (>10%) overshoot, occurred over the interval 0045–0100 MDT (and before the leeward 2D sonic anemometers were installed). It does not satisfy the selection criterion $u_* \geq 0.1$ m s^{-1} and has been included only to indicate the necessity for rigorous selection criteria: the 3D sonic anemometer gave values ($u_* = 0.029$ m s^{-1} and $L = -1.2$ m) that were grossly incompatible with the mast profiles; for example, the thermocouples indicated a strongly stable temperature profile, $T(4.25) - T(0.34) = 5.44°$ C and the bulk Richardson number was $\mathrm{Ri}_b = +0.16$. Thus it is possible, and even likely, that the overshoot effect in the current experiments is not real.

In Fig. 9, it is notable that at leeward positions $x/h = (2, 4, 6)$ there is a monotonic improvement of the shelter factor (falling relative wind speed) *as approach speed increases*, whereas in the neutral limit, we are accustomed to thinking that normalized wind speeds about a windbreak ought to be invariant, for fixed orientation (this is why we normalize: to define a pattern that, as far as is possible, is independent of the absolute wind speed). Of course, increasing approach speed S_0 correlates with increasing $|L|$ and decreasing bulk Richardson number. Plotting fractional wind reduction of the individual 15-min runs against Ri_b and against S_0 (Fig. 10) results in a noisy pattern, in either case. The cautious interpretation of Fig. 10 is that (at this large angle of obliquity, $\beta' = 60°$) stability exerts no clear influence unless $\mathrm{Ri}_b > 0.02$ or roughly $S_0 < 2$ m s^{-1}. Observed $\Delta S/S_0$ ordered slightly better against the bulk Richardson number than against h/L, essentially because of the propensity of sonic-anemometer-derived u_* and L to be wrong at small u_*. The region across which stability exerts an influence can be expressed as $|L| < 10h$.

d. *Summary of the influence of obliquity and stratification*

Figure 11 combines several of the previous transects to summarize the influence of obliquity under neutral stratification and indicates that shelter effectiveness is reduced[3] in oblique winds, with the point of best shelter ($\check{x}$) moving closer to the windbreak. Similar field observations have been given by Seginer (1975b, his Fig. 5) for several values of h/z_0 and a value of k_{r0} that, while not given, must have been similar to the current fence; because (irrespective of h/z_0) Seginer's minimum relative speeds, for perpendicular incidence, were $(S/S_0)^{\min} \approx 0.38$, implying [from Eq. (3)] that $k_{r0} \approx 2.8$. Seginer gave a strikingly regular set of transects at 5° intervals of obliquity, by fitting empirical curves $S/S_0 = f(x/h, \beta)$ to his (more scattered) raw observations. Note that because of the nature of his smoothing procedure, Seginer not only obtained regular curves, but also, to some extent, dictated the shape of the transects. Richards et al. (1984, their Fig. 4) also have given wind

[3] Computations by Wang and Takle (1996) for a ''low density'' shelterbelt of finite width $h/2$ gave an *increased* depth of the wind reduction curve (more effective shelter) in the near lee, for oblique winds. Although that effect has been observed neither for tree windbreaks (Nord 1991) nor for fence flows, as Wang and Takle argue, its putative existence may hinge on the variation of ''effective foliage density'' with pathlength of the wind through the shelter, which (for thick shelterbelts) is increased in oblique winds.

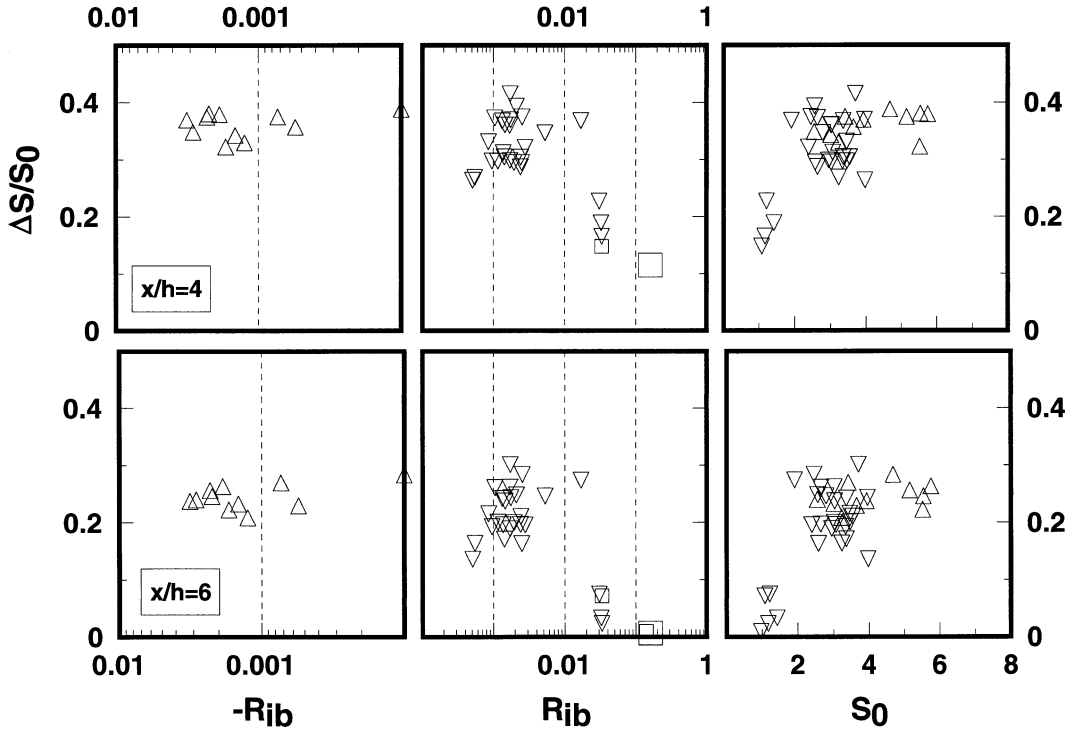

FIG. 10. Sensitivity to stability (bulk Richardson number Ri_b) and approach wind speed S_0 (m s^{-1}) of the fractional wind speed reduction $\Delta S/S_0$ according to the cup anemometers at $x/h = (4, 6)$ for an approach wind direction 60° ± 10° away from the normal to the fence. Upward (downward) triangles denote unstable (stable) stratification. Square symbols denote runs for which $u_* < 0.1$ m s^{-1}, and the large squares at $Ri_b = +0.16$ correspond to the run for which the 3D sonic anemometer (erroneously) gave $u_* = 0.029$ m s^{-1} and $L = -1.2$ m.

reduction curves in oblique flow about a fence, derived from wind-tunnel simulations.

It is interesting to compare Fig. 11 with the corresponding data of Nord (1991, her Fig. 11) for oblique winds about a multiple-row shelterbelt of birch and spruce. Overall, the impact of oblique flow is similar for the natural and artificial windbreaks, although in contrast to the case of a thin fence Nord observed that (even in near-neutral stratification) an oblique wind about the natural shelterbelt resulted in speeds exceeding the distant reference, both upwind and downwind. It is not obvious to what factor(s) this distinction (between the fence and tree windbreaks) is attributable, but perhaps irregularity in the heights of the trees encourages secondary flows that enhance downward momentum transfer.

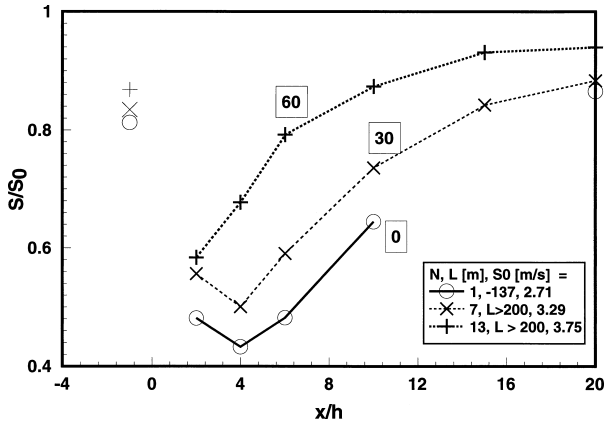

FIG. 11. Transects of relative wind speed S/S_0 from the cup anemometers, under near-neutral stratification, as a function of the (upwind) orientation of the mean wind β' (no cups on the anemometer at $x/h = 15$, during the perpendicular run). Here, as always in this paper, the x axis is perpendicular to the fence.

An alternative view of the effect of wind obliquity is given by Fig. 12, which examines the fractional wind reduction $\Delta S/S_0$ at fixed positions ($x/h = 4$, 6, 10, 15, and 20), as a function of the approach wind direction β. In this case, the data have been only loosely sorted ($|L| \geq 20$ m, $S_0 \geq 1$ m s^{-1}), and some fraction of the dispersion of points associated with fixed (β, x/h) is attributable to the nonneglible influence of stratification (it is interesting to note that the relative wind speeds from the cup and sonic anemometers do not differ systematically across the bulk of these data at $|L| \geq 20$ m). The fitted curves,

$$\Delta_S(x;\, \beta',\, L) = \Delta_S(x;\, 0,\, L)\, \cos^{x/4h}(270° - \beta), \quad (8)$$

prove that the simple cosine attenuation expressed by Eq. (6) is not correct at all downwind distances (this was already concluded in section 3c) while neither is a "$\cos^2\beta'$" law correct. As interpretive guidelines only,

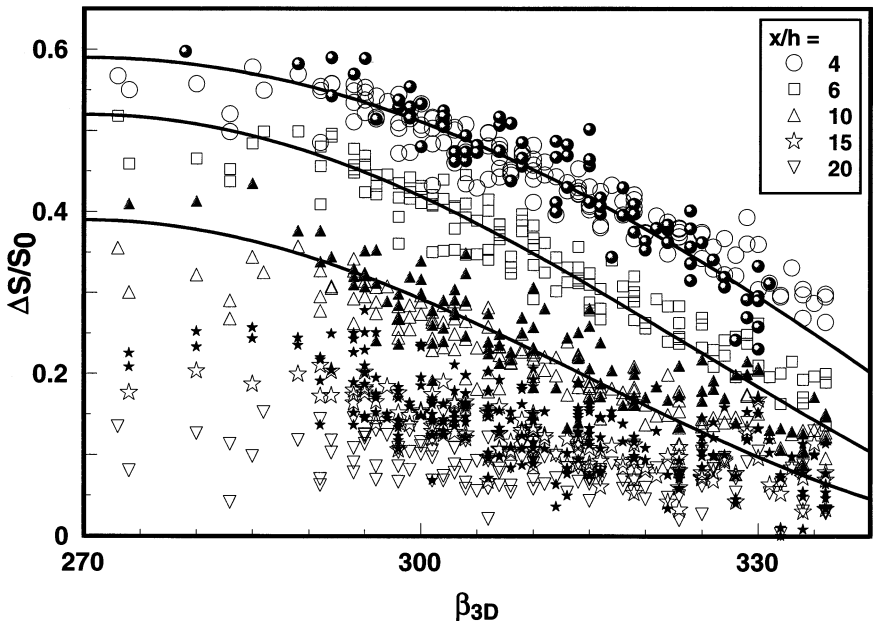

FIG. 12. Variation of the fractional wind reduction, at the specified distances x/h down the normal to the fence, as a function of the (upwind) orientation of the mean wind; comparison of open symbols (cup anemometers) and solid symbols (2D sonic anemometers) suggests there is no systematic *excess* overspeeding by the leeward cups for these conditions of stratification. Data selection criteria are $|L| \geq 20$ m and $S_0 \geq 1$ m s^{-1}. The solid lines are an empirical formula [Eq. (8)] given in the text.

Wang and Takle (1996) gave exploratory heuristic arguments (both of which they recognized as implausible) for both the cosine and cosine-squared attenuation laws, arguments that depended on the relative efficiency with which the shelter diminishes the normal and parallel components of the mean velocity. It seems unlikely that a simple ''macroscopic'' law, valid across all artificial and natural shelterbelts, determines the relative efficiency with which normal and parallel components are attenuated, because observations show that at the downwind edge of a thick natural shelterbelt the parallel velocity component essentially vanishes (Nord 1991; Tuzet and Wilson 2004, unpublished manuscript), whereas across a simple planar fence there is a discontinuous (but *incomplete*) rotation of the emergent wind direction toward the normal because of (incomplete) absorption of the transverse momentum flux ($\overline{u}\,\overline{v} + \overline{u'v'}$) incident on the upwind side.

A further point relative to Fig. 12 is the low sensitivity of fractional wind reduction to the obliquity angle β, in near-normal flow. This effect is obviously related to the ''flatness'' of $\cos(\beta')$ for small β', but the practical importance is that one may fairly say that the windbreak is almost equally (and maximally) effective over the wide range $\beta' = \pm 30°$. This is consistent with the findings of Wilson (1997) regarding the mean pressure field, which likewise was found to be largely indifferent to the approach wind direction over this range.

Regarding the influence of stability, the preceding results (and particularly Fig. 10) leave an impression that it is weaker in oblique flows than for the perpendicular case. This impression is reinforced by Fig. 13, which shows that fractional wind speeds S/S_0 at $x/h = (4, 10)$, even when tightly sorted for mean wind direction ($|\beta' - 45°| \leq 10°$), do not form a systematically organized pattern relative to stratification h/L (no better organization was apparent vs Ri_b). To restate the point, Fig. 13 indicates that even when filtered very selectively for mean wind direction and stratification, relative mean wind speed at a fixed location relative to the barrier is *not invariant* [here it is pertinent to quote Dyer and Bradley (1982) in the context of stability of micrometeorological statistics: ''evidence is mounting that the atmosphere does not follow the averaged laws at all places and all times even over an excellent site'']. Is there an ''uncontrolled'' external parameter whose variation from run to run might explain the residual scatter of 15-min averages S/S_0 at fixed h, z_0, k_{r0}, x/h, z/h, h/L, and β', assuming this (residual scatter) reflects a ''real'' influence and not just instrumental error? It is familiar that the boundary layer depth δ influences the horizontal velocity statistics, but it is not obvious how that influence could modulate the mean pattern of the winds about this barrier more emphatically in oblique than in normal winds. A possibility that should be mentioned, bearing in mind that in the wind-tunnel tests only *high-velocity* streams (5–10 m s^{-1}) were forced through the screen, is that the resistance coefficient k_{r0}

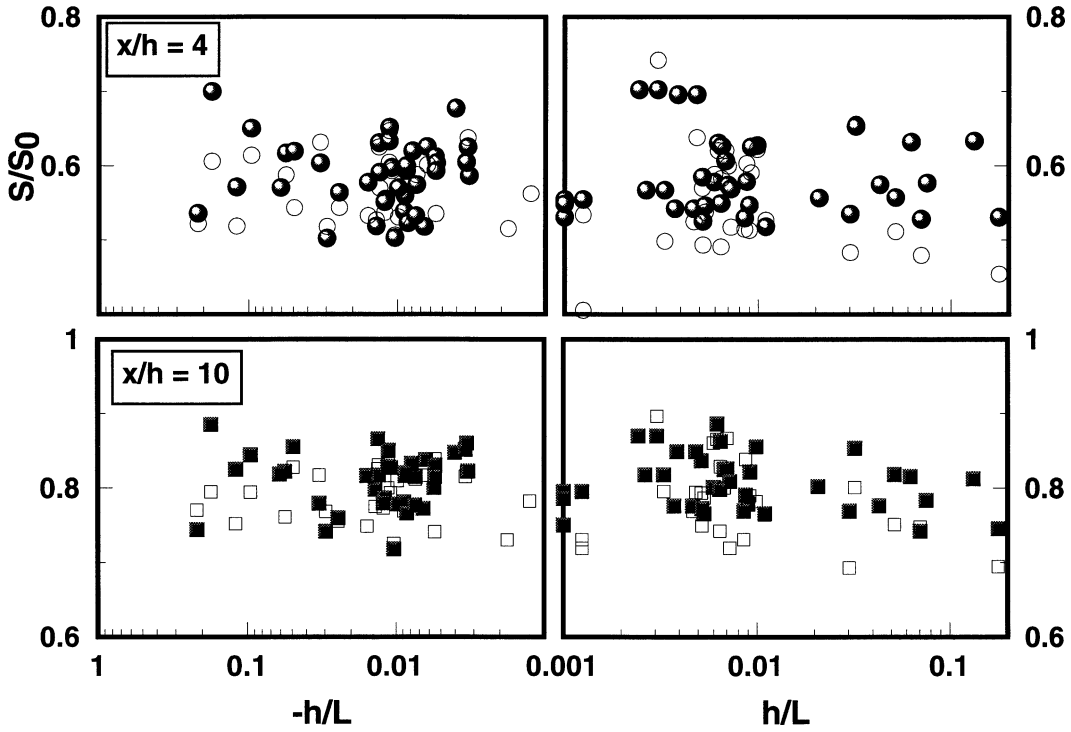

FIG. 13. Relative wind speed plotted against stratification for oblique winds at $|\beta' - 45°| \leq 10°$. Cup anemometer data (solid symbols) are for $S_0 \geq 1$ m s^{-1} and $u_* \geq 0.1$ m s^{-1}; sonic anemometer data (open symbols) are plotted irrespective of wind speed.

is not Reynolds number independent over the range of conditions encountered in the field. A more disturbing possibility (because random, unknowable, and irreproducible) is that it may have been unwarranted to tolerate (or neglect) what seemed to be minor derangements of the geometry of the barrier. Strong overnight winds once or twice tilted (some) posts by up to about 10° away from the vertical direction, and although such extreme irregularities were corrected promptly, no attempt was made to filter out observations from the corresponding intervals. Also, in truth no criterion exists to justify the supposition that mean wind orientations across the range $35° \leq \beta' \leq 55°$ can be considered to be equivalent, permitting many runs to be ''pooled.''

e. An empirical wind reduction curve: Potential shelter

Wilson et al. (1990) gave an analytical solution for a simplified windbreak flow (small k_{r0}, no upwind shear) that neglected the downwind recovery (viz., no turbulent vertical momentum transfer, or loosely ''no diffusion''),

$$\frac{\Delta S(x, z)}{S_0} = \frac{k_{r0}}{2\pi}\left(\text{atan}\frac{x}{z - h} - \text{atan}\frac{x_0}{z - h} - \text{atan}\frac{x}{z + h} + \text{atan}\frac{x_0}{z + h}\right), \quad (9)$$

where $x_0 < 0$ is a large upstream distance (say, $-20h$). According to this formula, the minimum leeward wind speed is $(S/S_0)^{\min} = 1 - k_{r0}$ (i.e., the perturbation in relative wind speed is numerically equal to k_{r0}), while fractional wind reduction right at the fence is exactly $(1/2)k_{r0}$.

For finite k_{r0}, the amplitude of the relative wind curve is smaller than k_{r0}, and if the factor k_{r0} in Eq. (9) is replaced by the $k_{r0}/(1 + 2k_{r0})^{0.8}$ of Eq. (3), one obtains a reasonable fit to the observed relative wind curve over approximately the range $x/h < 5$ (see dashed line in Fig. 14). To factor in the (''diffusion driven'') downstream recovery, any number of empirical functions could be invoked, and (as an example) Fig. 14 shows that the formula

$$\frac{\Delta S(x, z)}{S_0} = \frac{1}{2\pi}\frac{k_{r0}(1 + 2k_{r0})^{-0.775}}{1 + \left(\dfrac{x/h - 3}{9}\right)^2} \times \left(\text{atan}\frac{x}{z - h} - \text{atan}\frac{x_0}{z - h} - \text{atan}\frac{x}{z + h} + \text{atan}\frac{x_0}{z + h}\right) \quad (10)$$

nicely replicates the observed relative wind curve for the neutral, perpendicular case. Equation (10), in which

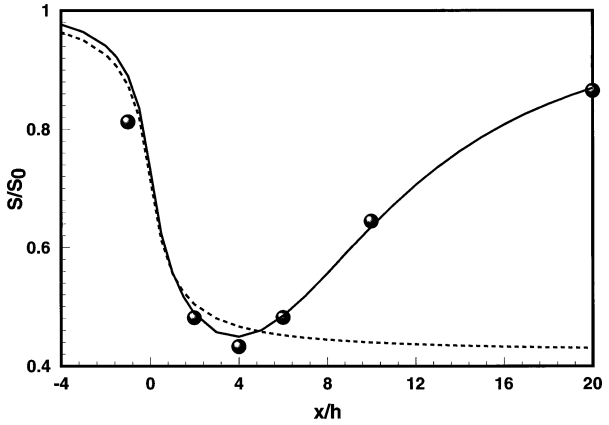

FIG. 14. Observations vs a semiempirical formula for the transect of relative wind speed S/S_0 across the windbreak in neutral winds at perpendicular incidence. The dashed line factors Eq. (3) into Eq. (9) to generalize the analytical no-diffusion solution for finite k_{r0}; the solid line is Eq. (10).

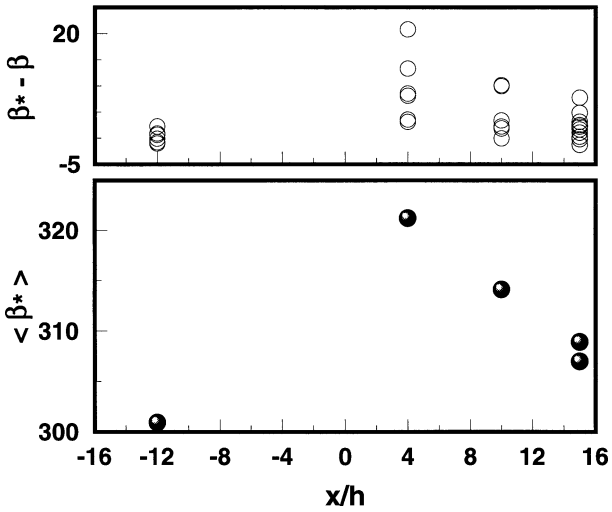

FIG. 15. Mean wind direction from the 2D sonic anemometers at $z/h = 1/2$ for six oblique, near-neutral runs ($|L| > 200$ m, $S_0 \geq 3$ m s^{-1}, and $|\beta_v - 300| \leq 5°$). (top) Open symbols give the run-by-run deviations between two alternative measures of the local mean orientation of the wind: $\beta_* = \arctan(\overline{v}/\overline{u})$ is the orientation of the mean wind, and $\beta = \overline{\arctan(v/u)}$ is the mean orientation of the instantaneous wind. (bottom) Solid symbols give the ensemble mean direction $\langle\beta_*\rangle$ across all six runs.

the arbitrary dimensionless constants (3, 9) control the onset and rapidity of the recovery, could be called the ''potential shelter'' curve for a thin porous barrier. However, it remains to be seen whether the given values of the free constants have generality.

The relative wind curve could have been obtained by modifying (for large k_{r0}, as above) a more complex analytic solution given by Wilson et al. (1990) that *did* retain the Reynolds stress divergence driving downwind recovery. However, that solution cannot be expressed in a single, simple formula.

f. Disturbance in wind direction

Changes in mean wind direction about a fence (Mulhearn and Bradley 1977) or shelterbelt (Nord 1991) are systematic and can be related (Wang and Takle 1995; Wilson and Flesch 2003) to the influence of the dominating pressure gradient normal to the windbreak[4] (and which within the shelter is oriented down the ''path of least resistance''). The 2D sonic anemometers provided both $\beta = \overline{\text{atan}\,(v/u)}$, the mean of the instantaneous wind directions, and $\beta_* = \text{atan}(\overline{v}/\overline{u})$, the orientation of the mean wind; the former is, in principle, equivalent to the signal β_v provided by a wind vane. Figure 15 gives the observed mean wind directions for an ensemble of six windy, neutral runs ($|L| \geq 200$ m) at 30° obliquity. Inspection of the mean velocity vectors (not shown) proved that not only $\overline{u}$ but also the along-fence component $\overline{v}$ was reduced in the near lee. However Fig. 15 demonstrates that in the near lee (although not right ''at'' the fence, where the bleed flow, that is, volume-averaged flow within the pores, deviates down the normal) the direction of the mean wind (β_*) deviates *away* from the normal to the fence, and this, of course, implies that $\overline{u}$ is reduced more than is $\overline{v}$ [this deviation away from the normal had earlier been noted by Mulhearn and Bradley (1977), and others]. One intuitively expects the resistance of a thin, planar fence to be ''felt'' more by the normal component u than the parallel component v, and that expectation is consistent with the sharp step in pressure across the fence, from an excess on the upwind to a deficit on the downwind edge; indeed the no-diffusion analytical treatment by Wilson et al. (1990) proves that the pressure gradient is almost *wholly* responsible for creation of the velocity deficit (the convergence-driven advection term $\overline{w}\,\partial\overline{u}/\partial z$, neglected in the analytical treatment, also plays a small role).

Figure 15 also shows that in the lee of a windbreak the difference ($\beta_* - \beta$) between the two definitions of mean wind direction may be large, up to 20° for the current selection of oblique, neutral winds. The mean (β) of the instantaneous wind directions was always much closer to the (upwind) mean vane direction than was the direction β_*. A criterion limiting ($|\beta - \beta_*|$) would presumably have reduced the statistical scatter in wind statistics within any given ''bin'' (narrow range in β, L), but such enhanced selectivity, even if the volume of experimental data made it practicable, might risk giving an unrealistic idea of the degree of ''tidiness'' or ''reproducibility'' of shelter winds. In principle, this

[4] For the near-leeward region behind a fence where wind turns away from the normal, Wilson and Flesch neglected to mention the most obvious factor: that the adverse normal pressure gradient works to the extinction of the normal component in that region. However, it may be wrong to assume the nonexistence of a *parallel* pressure gradient $\partial\overline{p}/\partial y$ that could develop in oblique flow about a long but finite barrier in reaction to the loss of parallel (y) momentum to the windbreak.

selectivity ought to be equivalent to a selectivity vis-à-vis the upwind standard deviation of wind direction, and this (again, in principle) ought to correlate with the MOST scales. However, the reality is that the ensemble of atmospheric states (upwind, ''undisturbed'') corresponding to fixed (u_*, L, and boundary layer depth δ) is *not* homogeneous.

g. Influence of the windbreak on level of turbulence

Figure 16 gives transects, for increasingly oblique mean wind, of the normalized standard deviations as measured by the 2D sonic anemometers, for the velocity components in the directions normal (u) and parallel (v) to the fence, that is, $\sigma_u(x, h/2)/\sigma_u(-\infty, h/2)$ and the equivalent for v. Recall that no evidence was found that standard deviations from the 2D sonic anemometers are biased, and recall also that random sampling errors will have been diminished by averaging together 15-min (normalized) transects for Fig. 16.

For a perpendicular mean wind, in the lee of the fence σ_u is reduced out to about $x/h \approx 15$, while apparently only in the near lee is σ_v reduced: the quiet zone is broader for normal fluctuations than for parallel fluctuations, a point that does not seem to have been remarked from earlier studies of turbulence about a simple porous barrier and that have focused on the normal component. The short range of reduction of σ_v is consistent with earlier observations (Wilson 1987, his Fig. 6) in the lee of a somewhat different type of fence, which showed a full recovery of σ_v by $x/h \sim 7$. The paucity of available runs with perpendicular winds prevents any detailed comment on the influence of stability, but it does seem that intense instability does not result in a very different transect than does moderate instability.

The pattern in σ_u and σ_v is not very different in moderately oblique flow ($\beta' = 30°$), the only point of note being that in the single period shown with stable stratification, σ_v is definitively larger in the middle lee than it is upstream. Even in very oblique winds the quiet zone is still seen in the u fluctuations (normal to the fence) while fluctuations parallel to the windbreak are only slightly suppressed in the near lee and—under stable stratification—contain more energy in the mid- and far lee than upstream.

Differing heights of the two 3D sonic anemometers ($z = 2$ m and $z = h = 1.25$ m, upstream and downstream, respectively) prevented definitive assessment of the influence of the windbreak on the standard deviation σ_w of the vertical velocity. However, in normal and in moderately oblique flow the normalized ratios σ_w/σ_{w0} were not strongly stability dependent across the range $|L| >$ 10 m (i.e., when extreme stratification was excluded), and their values, falling within the limits 1.1–1.5 and 1.2–1.6 at $x/h = 2$ and 10, respectively, were broadly consistent with the profile of σ_w (along $z/h = 1$ behind a uniformly porous fence of different construction) given by Wilson (1987, his Fig. 5) for very weakly unstable stratification. The results here suggest Wilson's (1987) linear interpolation of σ_w/σ_{w0} between its measured values at $x/h \approx 1.5$ and 3 may have been unwarranted.

h. Total kinetic energy of the wind

Signals from the 2D sonic anemometers were processed to give the mean square horizontal speed, defined as $V^2 = \overline{u^2} + \overline{v^2} = \overline{u}^2 + \overline{v}^2 + \overline{u'^2} + \overline{v'^2}$. This differs in general from the square (S^2) of the mean cup wind speed $S = \sqrt{u^2 + v^2}$, also measured directly by the 2D sonic anemometers, except when the turbulence intensity is sufficiently low, in which case a binomial expansion of S yields

$$\mathrm{Lim}_{(\overline{u'^2},\overline{v'^2}\ll Q^2)} S = \mathrm{Lim}_{(\overline{u'^2},\overline{v'^2}\ll Q^2)} V = Q\left(1 + \frac{\overline{u'^2} + \overline{v'^2}}{2Q^2}\right), \qquad (11)$$

where $Q^2 = \overline{u}^2 + \overline{v}^2$. Thus no definite value for S/V can be expected, even in undisturbed flow. The current observations at $z = 0.62$ m and in nearly perpendicular winds gave $0.9 \leq S/V \leq 1$ in the upwind region, with slightly smaller values (clustering around 0.9) in the near lee.

Figure 17 gives transects of V^2, normalized on the value at the reference 2D sonic anemometer. The picture here for this ''totalized'' wind energy reduction is very simple: in perpendicular flow the mean square velocity is sharply reduced, and it recovers regularly on a distance of order $20h$. In regard to the factors ''driving'' this compound statistic, according to MOST, in neutral stratification in the upwind flow the contributions to V^2 are in the ratio $\sigma_u^2/\overline{u}^2$, where

$$\frac{\sigma_u}{\overline{u}} = \frac{c_u u_*}{(u_*/k_v)\,\ln(z/z_0)}, \qquad (12)$$

with von Kármán constant $k_v = 0.4$ and $c_u \approx 2$. This gives $\sigma_u/\overline{u} \approx 0.2$ at the height of the transects of Fig. 17, and so these transects probably reflect mainly the influence of changes in mean velocity. Of course, this is not to say alteration in the level of turbulence is insignificant as far as its consequences go—because time variability of the wind can cause damaging plant motion.

4. Conclusions

Evidence has been given that good-quality cup anemometers (with a distance constant of 1.5 m or shorter) may be used to measure the pattern of mean wind speed around a windbreak in neutral and moderately stratified winds, the overspeed factor in the disturbed leeward flow not deviating too seriously (if at all) from the value (for these cup anemometers, circa 8%–10%) in undisturbed winds. However, one cannot rule out the possibility that in these experiments the leeward cup ane-

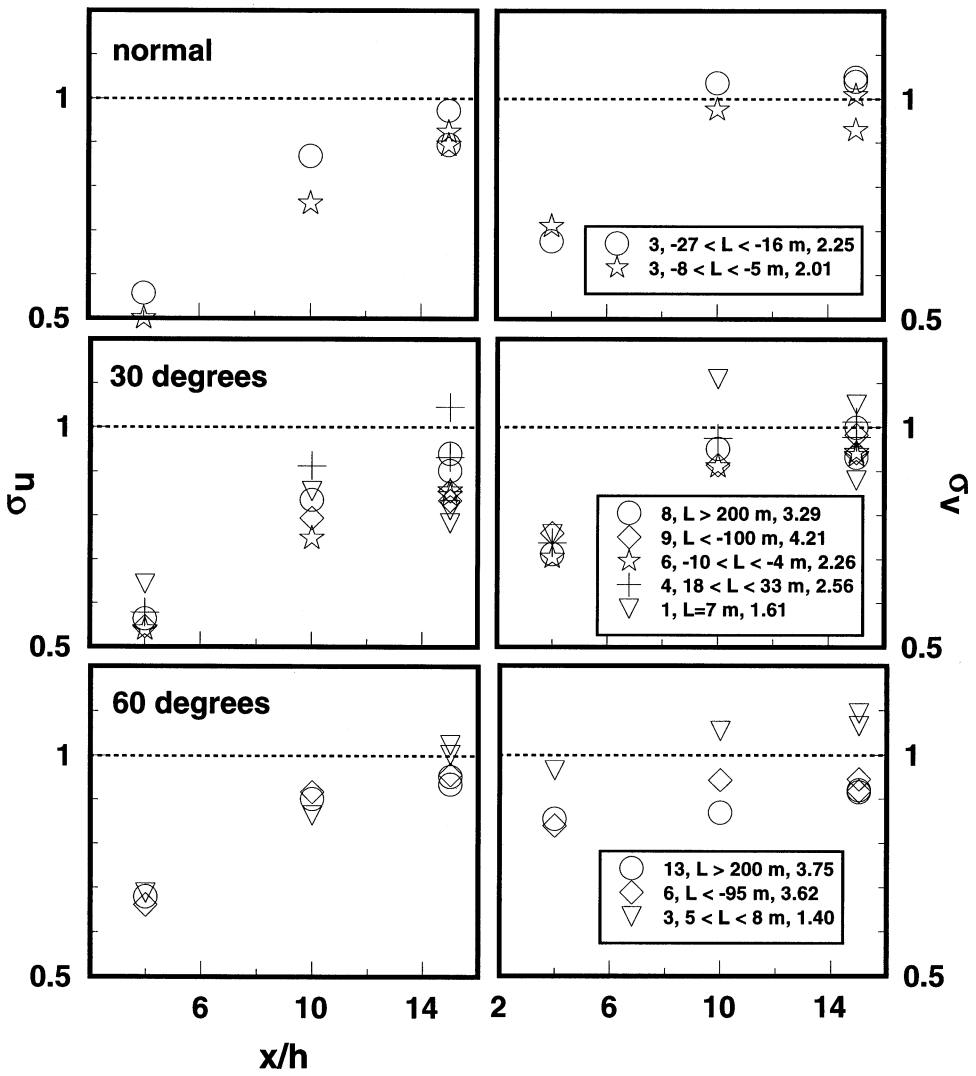

FIG. 16. Selected transects of the normalized standard deviations σ_u/σ_{u0} and σ_v/σ_{v0} of the components u and v (respectively, normal and parallel to the fence) as determined by the 2D sonic anemometers, for mean wind at three orientations relative to the normal to the fence.

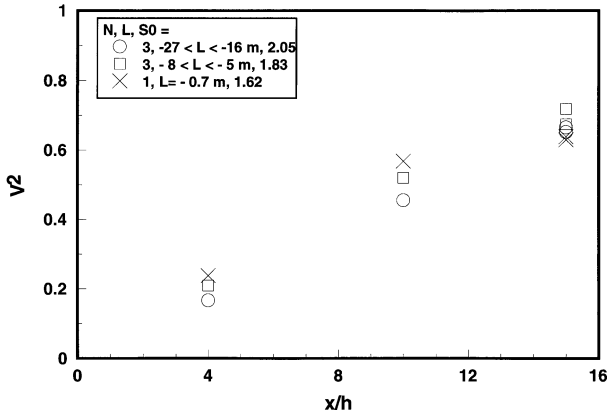

FIG. 17. Transects of mean-square wind speed $V^2 = \overline{u^2} + \overline{v^2} = \overline{u}^2 + \overline{v}^2 + \overline{u'^2} + \overline{v'^2}$, normalized by the upwind value, for periods with mean wind normal to the fence.

mometers oversped by *more* than 10% during strong and extreme stratification. To make further progress in defining the ''reality'' of a windbreak flow of this general type, and in particular the influence of extreme stratification (tending to correlate with light winds), it will be critical to select suitable vector wind sensors that must be precisely calibrated and capable of being sampled rapidly.

To arrive at well-ordered transects of wind reduction in the lee, it is crucially important to select only periods during which wind direction relative to the fence is known with certainty; in this respect the 2D and 3D sonic anemometers were vital, in that they allowed one to recognize a period in which the wind vane had crossed its dead band. It must be admitted, however, that wind speed transects organized according to the obliquity of the mean flow are to a certain extent arti-

ficial, because the decision as to what range (here $\pm 10°$) of mean wind directions to include is arbitrary, and instantaneous wind direction will have ranged far more widely than the interval chosen. It is disappointing to note the scatter on some of these figures, for example, Figs. 10 and 13, despite all attempts to order the nondimensionalized observations along the familiar ''axes of sensitivity'' (stability; obliquity) and to eliminate periods for which instrumental errors might be expected. Is this simply a question of inadequate averaging for reliable determination, or has one failed to find the right way to organize the data; that is, has one not identified all the key scaling variables in shelter flow? In fact the scatter would have been far greater if the selection criteria had been relaxed: for example (see Fig. 9) removal of the criterion $u_* \geq 0.1$ m s^{-1} would have admitted a run at $\beta' = 60°$, in which lee wind speed exceeded the reference upwind value by over 10%.

In this type of flow the discretion of the analyst (and the character of the instruments) may largely determine the view portrayed; if u_* is small and obliquity (β') is large, an averaging interval may include periods of wind reversal (downwind side temporarily upwind), in which case downwind wind speeds exceeding those upwind (i.e., overshoot) may be strictly real, albeit an artifice of the averaging: averaging may *disguise*, rather than reveal, cause and effect. When relationships between wind statistics fail to be ''orderly'' under the paradigm guiding the analysis, comprehensibility may need to be be sought by some other strategy. In this analysis a rudimentary type of ''conditional sampling'' has been used (binning with respect to ''external'' factors, obliquity and stratification), but perhaps to see more definitive ordering the sampling conditions need to be refined (e.g., one might register time series for all instruments and perform conditional sampling based on the low-pass-filtered field of wind direction).

The patterns seen here in mean wind speed reduction (shelter), as a function of obliquity and of stability, qualitatively resemble those seen in earlier studies, although Seginer's correction for the influence of unstable thermal stratification in perpendicular winds does not carry over to these (similar) observations. Perhaps the greatest novelty—and perplexity—of the data is that no very systematic influence of stratification could be distinguished, in very oblique winds. For the neutral case at a small angle of obliquity, simple formulas [Eqs. (3) and (7)] once again prove able to diagnose the degree of wind reduction in the near lee, as a function of resistance coefficient. On the evidence of these measurements the resistance coefficient k_{r0} *alone* determines what one might call the *potential shelter* provided by a long, thin, porous windbreak, across the wide range of incident wind directions for which some protection is expected, and stratification of either sign renders a given windbreak less effective. This is comprehensible on the unstable side as the consequence of stronger downward mixing of momentum into the leeward flow. On the stable side, perhaps the mechanism is that with increasing stability the jet over the windbreak is confined closer to ground, accentuating the mean shear, and so promoting faster recovery.

With regard to the practice of shelter, these results, along with many earlier studies of windbreaks, emphasize the distinction that must be made between windbreaks intended to protect crops and windbreaks intended for the comfort of animals (e.g., pine windbreaks of southern New Zealand, protecting wet sheep and lambs from cold winds during springtime storms that may coincide with lambing). In oblique winds only a narrow region may be sheltered, and if the wind blows over a windbreak corner the situation is even worse (Wilson and Flesch 2003). Animals will move, however, to whatever location behind a windbreak best pleases them.

Seginer (1975b) closed his elegant paper on shelter winds by remarking, ''The results, while they do not reveal any unexpected behavior, add to the meager empirical information on the subject. In due course they may be used to check on calculational results of flow around windbreaks.'' To this paper, almost 30 years later, those same words apply. The companion paper (Part II) will take up the subject of calculation, and so it is appropriate to end by emphasizing that (according to these observations) the similarity class of *experimental* shelter flows *may* need to be indexed by a longer list of characteristic scales and ratios and conditions (h/z_0, k_{r0}, h/L, β', etc.) than has been assumed necessary. Alternatively put, it seems nature does not offer one unambiguous field of wind statistics, for fixed values of these (few) characteristic scales. Even if it should be appropriate to regard this ambiguity (e.g., as to what is the ''real'' field of mean wind speed) as reflecting ordinary random sampling error, to be overcome by prodigious averaging within tightly selective classes [e.g., Bradley and Mulhearn (1983), who extracted 25 h of neutral data from 8 weeks of field work], this will rarely be possible in practice. It will seldom if ever be possible to evaluate micrometeorological wind models against ''*the* definitive field truth''!

Acknowledgments. This work has been supported by research grants from the Natural Sciences and Engineering Research Council of Canada (NSERC) and the Canadian Foundation for Climate and Atmospheric Sciences (CFCAS). I thank Drs. Keith Hage and Gerhard Reuter for their comments on the manuscript, and three anonymous reviewers who provided many useful suggestions.

APPENDIX

Sampling Errors of the 2D Sonic Anemometers

One measurement cycle for a Vaisala, Inc., WS425 wind sensor occupies 1 s so that under the particular sampling strategy used (SDI-12 digital output format

from Vaisala sonic anemometer, captured by CSI 23X datalogger using instruction ''P105'') the sampling interval for the collection of signals from all *eight* sonics could not be reduced below 8 s, resulting in just over 112 independent samples per each 15-min average.[A1] However, during the 1-s measurement cycle (of any one Vaisala sonic anemometer), flight-time measurements consume 150 ms (each of the three transducers transmits for 50 ms and receives for 100 ms) while signal processing and reporting uses the balance of the cycle: therefore one must ''consider each 1-s reading to be instantaneous'' (T. Calabria, Vaisala, Inc., 2004, personal communication). Given that sonic anemometers possess no mechanical inertia to smooth the wind signal, it follows that in the current measurements each 2D sonic anemometer provided a total of 112 instantaneous (unaveraged) wind estimates over the 15-min averaging interval.

According to the central limit theorem, we may therefore expect a sizeable sampling error of the mean. In specific terms, we may expect, with 95% probability, that the sampling error of the mean is less than $2\sigma_u/\sqrt{112}$, where σ_u is the standard deviation of the wind speed. If we estimate the latter as about 1 m s^{-1}, then with 95% probability, sampling error of the mean wind speed from the 2D sonic anemometers should be less than 0.2 m s^{-1}. Random sampling errors in the sonic mean wind speed of order 0.1 m s^{-1} are, therefore, to be expected, and this presumably explains the larger standard deviations of the ensemble of normalized profiles from the 2D sonic anemometers (Fig. 4) than of the cup profiles. Correspondingly, individual profiles from the 2D sonic anemometers were noticeably more ''ragged'' than those provided by the cups.

REFERENCES

Argete, J. C., and J. D. Wilson, 1989: The microclimate in the centre of small square sheltered plots. *Agric. For. Meteor.,* **48,** 185–199.

Bradley, E. F., and P. J. Mulhearn, 1983: Development of velocity and shear stress distributions in the wake of a porous shelter fence. *J. Wind Eng. Ind. Aerodyn.,* **15,** 145–156.

Dyer, A. J., and E. F. Bradley, 1982: An alternative analysis of flux–gradient relationships at the 1976 ITCE. *Bound.-Layer Meteor.,* **22,** 3–19.

Heisler, G. M., and D. R. Dewalle, 1988: Effects of windbreak structure on wind flow. *Agric. Ecosyst. Environ.,* **22/23,** 41–69.

Jacobs, A. F. G., and L. Wartena, 1987: Flow and turbulence around thin fences in perpendicular and oblique flow direction. *Neth. J. Agric. Sci.,* **35,** 7–20.

Laws, E. M., and J. L. Livesey, 1978: Flow through screens. *Annu. Rev. Fluid Mech.,* **10,** 247–266.

McAneney, K. J., and M. J. Judd, 1987: Comparative shelter strategies for kiwifruit: A mechanistic interpretation of wind damage measurements. *Agric. For. Meteor.,* **39,** 225–240.

McNaughton, K. G., 1988: Effects of windbreaks on turbulent transport and microclimate. *Agric. Ecosyst. Environ.,* **22/23,** 17–39.

——, 1989: Micrometeorology of shelterbelts and forest edges. *Philos. Trans. Roy. Soc. London,* **B324,** 351–368.

Mulhearn, P. J., and E. F. Bradley, 1977: Secondary flows in the lee of porous shelterbelts. *Bound.-Layer Meteor.,* **12,** 75–92.

Nord, M., 1991: Shelter effects of vegetation belts—Results of field measurements. *Bound.-Layer Meteor.,* **54,** 363–385.

Raine, J. K., and D. C. Stevenson, 1977: Wind protection by model fences in a simulated atmospheric boundary layer. *J. Ind. Aerodyn.,* **2,** 159–180.

Richards, P. J., E. F. Kay, D. Russell, and G. R. C. Wilson, 1984: Porous artificial windbreaks in oblique winds. Institute of Professional Engineers of New Zealand (IPENZ) Paper 67/84, Hastings, 1–10.

Seginer, I., 1975a: Atmospheric-stability effect on windbreak shelter and drag. *Bound.-Layer Meteor.,* **8,** 383–400.

——, 1975b: Flow around a windbreak in oblique wind. *Bound.-Layer Meteor.,* **9,** 133–141.

Wang, H., and E. S. Takle, 1995: Numerical simulations of shelterbelt effects on wind direction. *J. Appl. Meteor.,* **34,** 2206–2219.

——, and ——, 1996: On shelter efficiency of shelterbelts in oblique winds. *Agric. For. Meteor.,* **81,** 95–117.

Wilson, J. D., 1985: Numerical studies of flow through a windbreak. *J. Wind Eng. Ind. Aerodyn.,* **21,** 119–154.

——, 1987: On the choice of a windbreak porosity profile. *Bound.-Layer Meteor.,* **38,** 37–49.

——, 1997: A field study of the mean pressure about a windbreak. *Bound.-Layer Meteor.,* **85,** 327–358.

——, 2004: Oblique, stratified winds about a shelter fence. Part II: Comparison of measurements with numerical models. *J. Appl. Meteor.,* in press.

——, and T. K. Flesch, 2003: Wind measurements in a square plot enclosed by a shelter fence. *Bound.-Layer Meteor.,* **109,** 191–224.

——, and E. Yee, 2003: Calculation of winds disturbed by an array of fences. *Agric. For. Meteor.,* **115,** 31–50.

——, G. E. Swaters, and F. Ustina, 1990: A perturbation analysis of turbulent flow through a porous barrier. *Quart. J. Roy. Meteor. Soc.,* **116,** 989–1004.

Zhuang, Y., and J. D. Wilson, 1994: Coherent motions in windbreak flow. *Bound.-Layer Meteor.,* **70,** 151–169.

[A1] Other formats and sampling strategies may be available, and this comment is not meant to imply fault on the part of Vaisala or CSI.